Chemical Science

EDGE ARTICLE

View Article Online
View Journal | View Issue

Cite this: *Chem. Sci.*, 2019, **10**, 320

All publication charges for this article have been paid for by the Royal Society of Chemistry

Received 13th August 2018
Accepted 9th October 2018

DOI: 10.1039/c8sc03584a

rsc.li/chemical-science

A cell membrane-anchored fluorescent probe for monitoring carbon monoxide release from living cells†

Shuai Xu,‡[a] Hong-Wen Liu,‡[ab] Xia Yin,[a] Lin Yuan,[a] Shuang-Yan Huan*[a] and Xiao-Bing Zhang*[a]

Carbon monoxide (CO) acts as an important gasotransmitter in delivering intramolecular and intermolecular signals to regulate a variety of physiological processes. This lipid-soluble gas can freely pass through the cell membrane and then diffuse to adjacent cells acting as a messenger. Although many fluorescent probes have been reported to detect intracellular CO, it is still a challenge to visualize the release behavior of endogenous CO. The main obstacle is the lack of a probe that can anchor onto the cell membrane while having the ability to image CO in real time. In this work, by grafting a polar head onto a long and linear hydrophobic Nile Red molecule, a cell membrane-anchored fluorophore **ANR** was developed. This design strategy of a cell membrane-anchored probe is simpler than the traditional one of using a long hydrophobic alkyl chain as a membrane-anchoring group, and endows the probe with better water solubility. **ANR** could rapidly bind to the cell membrane (within 1 min) and displayed a long retention time. **ANR** was then converted to a CO-responsive fluorescent probe (**ANRP**) by complexation with palladium based on a metal palladium-catalyzed reaction. **ANRP** exhibited a fast response to CO with a 25-fold fluorescence enhancement *in vitro*. The detection limit was calculated to be 0.23 μM, indicating that **ANRP** is sensitive enough to image endogenous CO. Notably, **ANRP** showed excellent cell membrane-anchoring ability. With **ANRP**, the release of CO from HepG2 cells under LPS- and heme-stimulated conditions was visualized and the cell self-protection effect during a drug-induced hepatotoxicity process was also studied. Moreover, **ANRP** was successfully applied to the detection of intracellular CO in several cell lines and tissues, and the results demonstrated that the liver is the main organ for CO production, and that cancer cells release more CO from their cells than normal cells. **ANRP** is the first membrane-anchored CO fluorescent probe that has the ability to reveal the relationship between CO release and diseases. It also has prospects for the studying of intercellular signaling functions of CO.

Introduction

Endogenous carbon monoxide (CO), mainly produced by the degradation of heme by heme oxygenase (HO), plays an important role in the regulation of various physiological processes.[1–4] As a kind of lipid-soluble gas, intracellular CO can freely pass through the cell membrane, then diffuses to adjacent cells acting as a gasotransmitter,[5] and is finally excreted *via* the lungs.[6,7] For example, astrocytes employ CO as a messenger that diffuses to myocytes, causing cerebral arteriole dilation.[8] CO functions as a paracrine messenger molecule that causes hyperpolarization of circular smooth muscle cells.[9] And in diabetes, more CO diffuses from cells into the blood, causing elevated levels of exhaled CO.[10] These processes are always altered by pathological factors, such as severe sepsis and inflammation.[1,6] Thus, real-time monitoring of the release of CO from living cells is of great significance, to study its intercellular signaling functions and some related pathophysiological processes.

With advantages of high sensitivity, fast analysis and nondestructive detection, fluorescent imaging techniques have been widely used to analyze and image CO in biological samples.[11–23] Among them, a palladium-mediated reaction-based[24] CO fluorescent probe was first reported by Chang[11] and various CO fluorescent probes were successively designed by

[a]*Molecular Science and Biomedicine Laboratory, State Key Laboratory of Chemo/Biosensing and Chemometrics, College of Chemistry and Chemical Engineering, Collaborative Innovation Center for Chemistry and Molecular Medicine, Hunan University, Changsha, 410082, P. R. China. E-mail: syhuan@hnu.edu.cn; xbzhang@hnu.edu.cn*

[b]*Key Laboratory for Green Organic Synthesis and Application of Hunan Province, Key Laboratory of Environmentally Friendly Chemistry and Applications of Ministry of Education, College of Chemistry, Xiangtan University, Xiangtan 411105, P. R. China*

† Electronic supplementary information (ESI) available. See DOI: 10.1039/c8sc03584a

‡ These authors contributed equally to this work.

other authors based on this strategy.[17,19–21] However, all of these probes fail to locate on the cell membrane. So, it is still a big challenge to visualize in real time the release of CO from living cells, which will help researchers to better understand the release behavior and the intercellular signaling functions of CO.

The cell membrane is the boundary between a living cell and its environment, and many physiological processes including signal transduction and biomolecular transport occur on the cell membrane.[25] Installing a probe on the cell membrane provides the possibility of monitoring the release behavior of CO from living cells in real time. The fluorophore, which is highly lipophilic, tends to localize on the cell membrane *via* interaction with the phospholipid bilayer.[26] In previous work, long hydrophobic alkyl chains were always grafted onto the fluorophore to help the target probe anchor onto the cell membrane.[25,27–29] However, these probes have many drawbacks, such as poor water solubility and a tedious design process. Moreover, just grafting a long hydrophobic chain onto the probe cannot guarantee that this probe would anchor well onto the cell membrane. In the design of membrane-anchored probes, another characteristic of the cell membrane which needs to be taken into account is that it contains many negatively charged phosphate groups. Positively charged groups, which can interact with the phosphate groups of the cell membrane, will improve the ability of these fluorophores to anchor onto the negative cell membrane.[30]

Based on this knowledge, a cell membrane-anchored fluorophore (**ANR**) was designed by grafting a positively charged ammonium group onto a long and linear hydrophobic Nile Red molecule (Scheme 1). The advantageous features of **ANR** include high sensitivity and two-photon excitation with emission in the near infrared region. The design process was relatively simple, and the cell membrane was specifically stained by **ANR** with a long retention time over 60 min (Fig. S1†). Moreover, the complexing of the fluorophore with palladium based on a metal palladium-catalyzed reaction offers a convenient way to detect CO. Herein, by complexing **ANR** with palladium, a novel cell membrane-anchored fluorescent probe (**ANRP**) was designed and synthesized for real-time visualization of the release of CO from living cells (Scheme 1). The experimental results demonstrated that **ANRP** exhibited high selectivity and sensitivity to CO and could anchor well onto the cell membrane to monitor the release of CO from living cells under LPS- and heme-stimulated conditions. Moreover, **ANRP** was successfully applied to the detection of intracellular CO in several cell lines. **ANRP** was also used for imaging CO in liver tissues under two-photon excitation. These results indicated that the liver is the main organ for CO production and that cancer cells release more CO than normal cells.

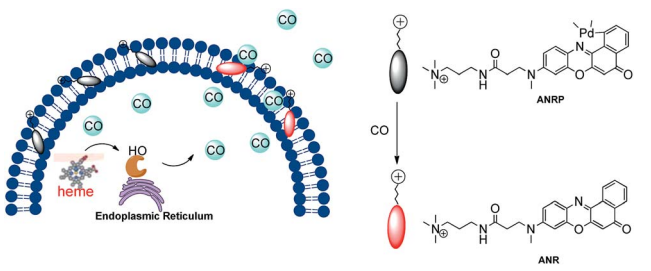

Scheme 1 Schematic illustration of the membrane-anchored probe for real-time monitoring of the release of CO from living cells.

Results and discussion

Before we attempted to construct a membrane-anchored CO fluorescent probe, a cell membrane-anchored fluorophore (**ANR**) was designed. Previous work has revealed that the hydrophobicity of general fluorophores assists in achieving desirable probe localization on the cell membrane.[26] And positively charged groups can interact with the phosphate groups of the cell membrane.[30] Thus, we postulate that a hydrophobic fluorophore, such as Nile Red, in combination with a positively charged ammonium group might be suitable for the development of cell membrane-anchored fluorescent probes. The structure of the carefully modified fluorophore (**ANR**) is shown in Scheme 1. In this molecule, the hydrophobic Nile Red tends to embed into the membrane, and the ammonium group pulls the whole molecule to prevent it from penetrating the cell membrane. The ability of **ANR** to target the cell membrane was studied in Fig. S1.† Moreover, when we grafted other positively charged groups such as a pyridinium salt or tetraethylammonium onto Nile Red, we were surprised to find that these two derivatives (**AeNR** and **ApNR**) could also stain the cell membrane (Fig. S2†). The ability of these compounds to stain the cell membrane may be attributed to their bipolar structure.[31] Our work may provide a convenient method to design a cell membrane-anchored probe. Next, **ANR** was chosen to construct a CO-responsive fluorescent probe (**ANRP**) by complexation with palladium based on a metal palladium-catalyzed reaction. Here, **AeNR** and **ApNR** are unsuitable for construction of a CO-responsive fluorescent probe due to relatively bulky groups at the 3-position of **AeNR** and **ApNR**, which make their palladacycle compounds unstable and have relatively strong background fluorescence (the data were not given). The synthetic route for **ANRP** was depicted in Scheme S1,† and the characterization of the new compounds is shown in the ESI.† Electron spin resonance (ESR) spectroscopy ($g \sim 1.9234$) and UV-vis-NIR spectra indicated that **ANRP** was a paramagnetic compound.

To confirm that **ANRP** was sensitive to CO, a chemical transformation experiment of **ANRP** in the presence of CO was performed by fluorescence spectroscopy in Dulbecco's phosphate-buffered saline (DPBS) (pH 7.4, DMSO/DPBS = 1 : 19, v/v). In this experiment, CORM-2 was used as the CO donor. As shown in Fig. 1a, **ANRP** showed very weak fluorescence in the absence of CO, and a gradual increase in fluorescence intensity at 650 nm could be observed after adding different concentrations of CO ranging from 0 to 100 μM to **ANRP** solutions. The fluorescence intensity of **ANRP** increased by 25-fold upon reaction with 100 μM CORM-2 for 30 min. A satisfactory linear correlation ($R^2 = 0.990$) between the fluorescence intensity and CO concentrations between the range of 5–25 μM was obtained (Fig. 1b). The detection limit was

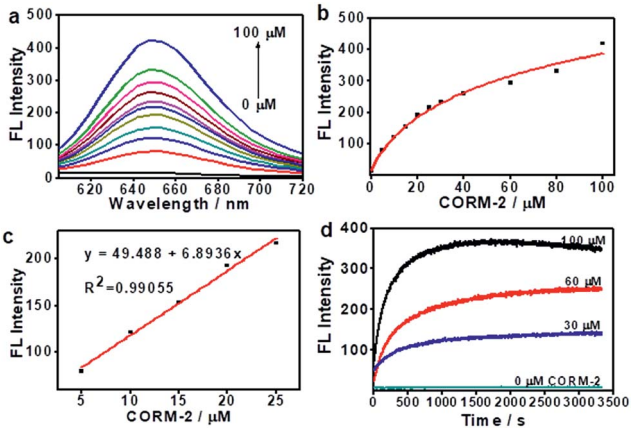

Fig. 1 The fluorescence response of ANRP (5 μM) towards CO in DPBS (pH 7.4, 5% DMSO). (a) Fluorescence emission spectra of ANRP with an increasing amount of CORM-2. (b) A calibration curve of ANRP to CORM-2; the curve was plotted with the fluorescence intensity at 650 nm *vs.* the CORM-2 concentration. (c) The linear relationship between the fluorescence intensity and the CORM-2 concentration. (d) Kinetic curves of ANRP reacted with CORM-2 at different concentrations (0, 30, 60, and 100 μM).

calculated to be 0.23 μM (~6.4 ppb) for CO (3σ/slope), indicating that **ANRP** is sensitive enough to image endogenous CO in living cells or tissues with a concentration range of 100–500 ppm. The reaction mechanism of **ANRP** towards CO was studied by mass spectroscopy (Fig. S3†) and HPLC (Fig. S4†).

The effect of pH on the reaction was also studied (Fig. S5†). In the pH range 4 to 10, the fluorescence intensity of **ANRP** had no obvious change, suggesting that the probe was stable in a wide range of pH values. After treatment with 50 μM of CORM-2, the fluorescence intensity at 650 nm exhibited a great enhancement in pH 7.4 buffer solution, which displayed the feasibility of using this probe in a physiological environment.

The response curves of **ANRP** reacting with CO at different concentrations (0, 30, 60, and 100 μM) were examined. After treatment with various concentrations of CO, the fluorescence intensity of **ANRP** at 650 nm increased rapidly within 20 minutes, and reached a plateau after 30 minutes (Fig. 1d). In the absence of CO, no obvious change in fluorescence intensity at 650 nm was observed. These results demonstrated that **ANRP** is suitable for the rapid detection of CO and tracking the fluctuation of CO content.

The specificity of a probe always determines whether it can be applied to complex biological systems. Considering this, the selectivity of **ANRP** to CO in the presence of various potentially interfering species was studied. As shown in Fig. S6,† only CO induced a large fluorescence enhancement at 650 nm, and other interfering species including reactive oxygen species (H_2O_2 and ClO^-), other reducing species (GSH and HS^-) and some metal ions (Fe^{2+} and Zn^{2+}) had little effect on the fluorescence of **ANRP**, indicating the high specificity of **ANRP** to CO.

Encouraged by the outstanding performances of **ANRP** *in vitro* mentioned above, we next applied **ANRP** to the detection of CO released from living cells. Before that, a CCK-8 assay was conducted to examine the cytotoxicity of **ANRP** to HeLa cells. As shown in Fig. S7,† relatively low cytotoxicity was observed when HeLa cells were cultured with various concentrations of **ANRP** for 24 h, which means that this probe is suitable for use in biological systems.

Next, we performed colocalization experiments using **ANRP**, a control probe **NR**, and a commercialized cell membrane tracker (Dio, a green color) to confirm the rationality of the design of our probe. After incubation with 5 μM **ANRP** for 30 min, the fluorescence in the cell membrane was weak. For a good imaging performance, the voltage used in this experiment was relatively higher than that used in other experiments. As shown in Fig. 2a, the red channel overlapped well with the green one, which demonstrated that **ANRP** can anchor onto the cell membrane well. As far as the control probe **NR** was concerned, most of the red **NR** signals appeared in the cells, and had poor overlap with the green Dio signals. These results also revealed the important role of the ammonium group in assisting the localization of **ANRP** on the cell membrane.

Then, imaging of exogenous CO through the HeLa cell membrane was performed. HeLa cells were cultured with 5 μM **ANRP** at 37 °C for 30 min, and then washed with DPBS three times. After that, 20 μM or 30 μM CORM-2 was added and the cells were further cultured for 30 min. As shown in Fig. 2b, the fluorescence on the cell membrane was brighter and more continuous than that on the cell membrane of the untreated cells, indicating that **ANRP** can anchor onto the cell membrane to image the release of CO from living cells.

We also applied this cell membrane-anchored probe to monitor the release of endogenous CO from HeLa, HepG2 and HL7702 cells. As shown in Fig. 3a, bright fluorescence on the cell membrane was observed in the three cell lines. Moreover, the fluorescence on the HepG2 cell membrane was brighter and more homogeneous than that on the HeLa and HL7702 cell membranes, indicating a higher amount of CO on the HepG2 cell membrane. The activation of **ANRP** was further confirmed by flow cytometry analysis (Fig. 3c). The results from the HeLa and HepG2 cell lines indicated that the liver is the major organ for CO production.[32] In another aspect, comparing HL7702 cells with HepG2 cells, HO is highly induced in cancer cells, leading

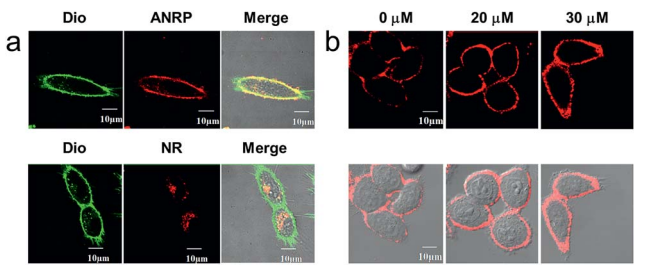

Fig. 2 (a) Colocalization experiments of ANRP (5 μM) and NR (5 μM) on the cell membrane of HeLa cells. Green channel (Dio, 10 μM): λ_{ex} = 488 nm, λ_{em} = 500–520 nm, red channel: λ_{ex} = 543 nm, λ_{em} = 600–700 nm. (b) Confocal fluorescence imaging of HeLa cells loaded with 5 μM ANRP before treatment with 0 μM, 20 μM and 30 μM CORM-2 for 30 min. λ_{ex} = 543 nm, λ_{em} = 600–700 nm.

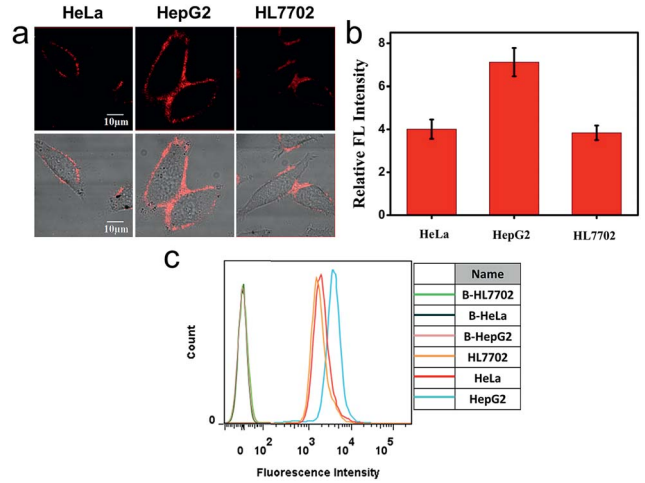

Fig. 3 (a) Confocal fluorescence imaging of HeLa, HepG2 and HL7702 cells loaded with 5 μM **ANRP**. (b) Relative fluorescence intensities of the different cells stained with **ANRP** in panel (a). (c) Flow cytometric analysis of **ANRP** (5 μM) fluorescence after incubation with HeLa, HepG2 and HL7702 cells (B = blank). λ_{ex} = 543 nm, λ_{em} = 600–700 nm.

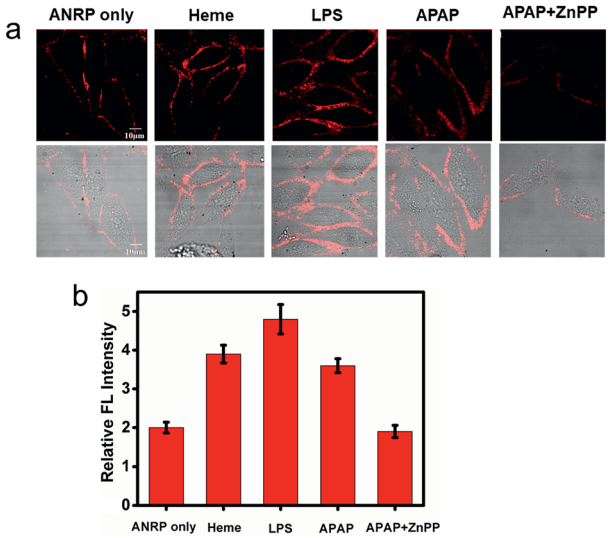

Fig. 4 Fluorescence images of **ANRP** (5 μM) in HepG2 cells under different conditions. Cells cultured with **ANRP** only, or pretreated with LPS (1 μg mL^{-1}) for 24 h, 20 μM heme for 8 h, 800 μM APAP for 12 h, 800 μM APAP and 10 μM ZnPP for 12 h, then **ANRP** at 37 °C for 30 min. (b) The relative fluorescence intensities of the HepG2 cell membranes in panel (a). λ_{ex} = 543 nm, λ_{em} = 600–700 nm.

to a higher degradation of heme, and resulting in more CO production and release.[33]

Real-time imaging of **ANRP** on the HepG2 cell membrane was further performed. The HepG2 cells were cultured with 5 μM **ANRP** for 30 min, and then washed with DPBS three times. After the treatment, 40 μM CORM-2 was added and the images were taken immediately. As shown in Fig. S8,† the fluorescence intensity of **ANRP** on the cell membrane increased gradually with increasing time and no obvious fluorescence was observed in the other regions of the cells including the cytoplasm when the incubation time reached 100 minutes. The results indicated that no signals diffused into cells and **ANRP** is suitable for the real-time detection of the extracellular release of CO.

Endogenous CO can be induced by many pathophysiological factors.[1] Using **ANRP**, the release of CO from HepG2 cells under different conditions was visualized. LPS and heme can both induce the overexpression of HO,[19] which can degrade heme into CO and bilirubin. In this experiment, HepG2 cells were stimulated by 1 μg mL^{-1} LPS for 24 h or induced by 20 μM heme for 8 h. Then, the HepG2 cells were cultured with 5 μM **ANRP** at 37 °C for 30 min. As shown in Fig. 4a, the fluorescence intensity of the pretreated cell membrane was stronger and the continuity was better, which suggested that more CO was released from heme- and LPS-treated HepG2 cells. In order to get more reasonable results, **ANRP** was first localized on the cell membrane and then the cells were stimulated by 20 μg mL^{-1} LPS or 30 μM heme for 4 hours. As shown in Fig. S9,† after LPS or heme stimulation, the fluorescence intensity on the membrane gradually increased with time, which indicated that **ANRP** could monitor carbon monoxide release as shown in Scheme 1. In addition, **ANR** was also used in co-incubation with LPS-pretreated HepG2 cells in order to confirm that LPS did not affect the behaviour of **ANRP** staining the HepG2 cell membrane (Fig. S10†). These results supported the hypothesis that **ANRP** could truly monitor the fluctuation of CO on the cell membrane during pathological or physiological processes.

Drug-induced liver injury (DILI) is a serious problem accounting for a substantial proportion of acute hepatitis.[34–36] Acetaminophen (APAP), a pain killer and fever reducer, always causes serious hepatotoxicity.[37] The main by-products of APAP metabolism are reactive radicals, which can lead to cell apoptosis and other acute liver damage.[35] Under oxidative stress, however, cells can avoid these oxidant effects by inducing the expression of HO to degrade heme into CO and bilirubin, which are well known antioxidants.[4] Based on this knowledge, we predicted that more CO might be released from APAP-stimulated HepG2 cells to provide cytoprotective effects. As shown in Fig. 4a, the fluorescence of the cell membrane of APAP-treated HepG2 cells was stronger than that of the control. To further confirm that the generation of CO was really induced by APAP, zinc protoporphyrin (ZnPP), an inhibitor of HO, was co-cultured with the APAP-treated HepG2 cells. As we can see, a weaker fluorescence intensity on the cell membrane was observed compared to APAP-treated HepG2 cells alone, suggesting that the increase of CO on the cell membrane was indeed induced by APAP. These experimental results support previous speculation that more CO is released from HepG2 cells in drug-induced hepatotoxicity processes to provide cytoprotective effects.

Near-infrared probes offer improved tissue penetration depth, and minimize background interference.[38–46] In this experiment, living organs including the liver, lung, kidneys, spleen and heart were isolated from living mice, and then treated with **ANRP** for 30 min. As shown in Fig. 5a, the fluorescence intensity in the liver was stronger than that in the lung, kidneys, spleen and heart, and no obvious background

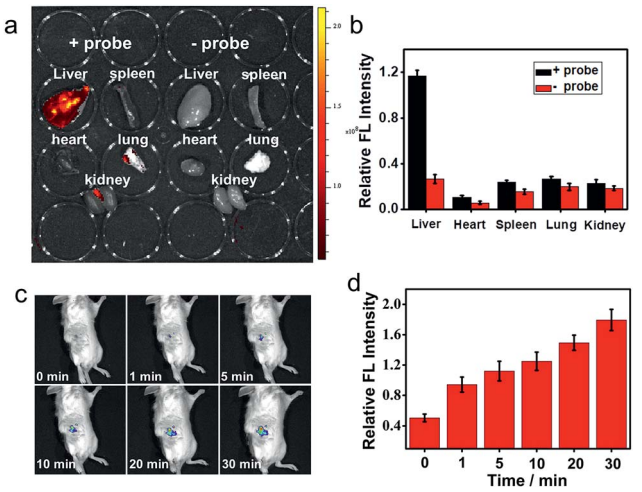

Fig. 5 (a) Fluorescence imaging of endogenous CO in the main organs using an *in vivo* imaging system. (b) The relative fluorescence intensities of the organs in panel (a). (c) *In vivo* fluorescence imaging of CO in living mice at different times. (d) The relative fluorescence intensity of the living mice in panel (c). λ_{ex} = 543 nm, λ_{em} = 570–650 nm.

fluorescence was observed in untreated liver tissue, which coincided with the cell imaging results and confirmed that the liver was the key organ for CO production.[32]

Next, two-photon fluorescence imaging of **ANRP** in liver tissue slices was performed. Two-photon fluorescent probes have the ability to realize deep tissue imaging and high imaging resolution.[47–55] Upon two-photon excitation at 780 nm, the fluorescence in **ANRP**-treated liver tissue slices at a depth of 5–90 μm was stronger than that in the PBS treated slices at the same depth (Fig. S11†). These results revealed that **ANRP** can be used for imaging CO in tissues under two-photon excitation.

Finally, the ability of **ANRP** to detect CO in living mice models was studied. After intraperitoneal injection of **ANRP** (30 μM, 50 μL in DMSO aqueous solution) in living mice, 100 μL of 100 μM CORM-2 was then injected in the same manner. The fluorescence signals were collected immediately. As shown in Fig. 5c, the fluorescence signal gradually increased with time and reached a plateau at 30 min. These results showed that **ANRP** is suitable to image CO in living mice.

Conclusions

In this work, by grafting a positively charged ammonium group onto hydrophobic Nile Red, a cell membrane-anchored fluorescent fluorophore **ANR** was developed. The design strategy may hold great promise for developing various cell membrane-anchored fluorescent probes. **ANR** can rapidly bind to the cell membrane, and displays a long retention time over 60 min. **ANR** was further converted to a cell membrane-anchored fluorescent probe **ANRP** by complexation with palladium. This modified probe exhibited high selectivity and sensitivity to CO and could particularly stain the cell membrane. **ANRP** was used to visualize the release of CO from living cells under LPS- and heme-stimulated conditions. With **ANRP**, we indicated that more CO was released from LPS-or heme-treated living cells. **ANRP** was further applied in drug-induced hepatotoxicity processes to study cell self-protection effects under oxidative stress by monitoring the release of CO. Using **ANRP**, we confirmed that the liver is the key organ for CO production, and that more CO is released from cancer cells. This membrane-anchored fluorescent probe may help to reveal the intercellular signaling functions of CO. It also allows for the study of the relationship between CO release and diseases.

Conflicts of interest

There are no conflicts to declare.

Acknowledgements

This work was supported by the National Natural Science Foundation of China (Grants 21675043, 21622504, 21735001, 21877029), and the Science and Technology Project of Hunan Province (2016RS2009, 2016WK2002).

Notes and references

1 E. O. Owens, *Clin. Biochem.*, 2010, **43**, 1183–1188.
2 M. Scharte, T. A. von Ostrowski, F. Daudel, H. Freise, H. Van Aken and H. G. Bone, *Eur. J. Anaesthesiol.*, 2006, **23**, 117–122.
3 R. Tenhunen, H. S. Marver and R. Schmid, *Proc. Natl. Acad. Sci. U. S. A.*, 1968, **61**, 748–755.
4 R. Gozzelino, V. Jeney and M. P. Soares, *Annu. Rev. Pharmacol.*, 2010, **50**, 323–354.
5 B. F. Moody and J. W. Calvert, *Med. Gas Res.*, 2011, **1**, 3.
6 R. Zegdi, D. Perrin, M. Burdin, R. Boiteau and A. Tenaillon, *Intensive Care Med.*, 2002, **28**, 793–796.
7 R. F. Coburn, R. E. Forster and P. B. Kane, *J. Clin. Invest.*, 1965, **44**, 1899–1910.
8 A. Li, Q. Xi, E. S. Umstot, L. Bellner, M. L. Schwartzman, J. H. Jaggar and C. W. Leffler, *Circ. Res.*, 2008, **102**, 234–241.
9 G. Farrugia and J. H. Szurszewski, *Gastroenterology*, 2014, **147**, 303–313.
10 P. Paredi, W. Biernacki, G. Invernizzi, S. A. Kharitonov and P. J. Barnes, *Chest*, 1999, **116**, 1007–1011.
11 B. W. Michel, A. R. Lippert and C. J. Chang, *J. Am. Chem. Soc.*, 2012, **134**, 15668–15671.
12 W. Feng, D. Liu, S. Feng and G. Feng, *Anal. Chem.*, 2016, **88**, 10648–10653.
13 S. Feng, D. Liu, W. Feng and G. Feng, *Anal. Chem.*, 2017, **89**, 3754–3760.
14 W. Feng, D. Liu, Q. Zhai and G. Feng, *Sens. Actuators, B*, 2017, **240**, 625–630.
15 W. Feng, J. Hong and G. Feng, *Sens. Actuators, B*, 2017, **251**, 389–395.
16 W. Feng and G. Feng, *Sens. Actuators, B*, 2018, **255**, 2314–2320.
17 Y. Li, X. Wang, J. Yang, X. Xie, M. Li, J. Niu, L. Tong and B. Tang, *Anal. Chem.*, 2016, **88**, 11154–11159.

18 K. Dhara, S. Lohar, A. Patra, P. Roy, S. K. Saha, G. C. Sadhukhan and P. Chattopadhyay, *Anal. Chem.*, 2018, **90**, 2933–2938.
19 K. Liu, X. Kong, Y. Ma and W. Lin, *Angew. Chem., Int. Ed.*, 2017, **56**, 13489–13492.
20 K. Zheng, W. Lin, L. Tan, H. Chen and H. Cui, *Chem. Sci.*, 2014, **5**, 3439–3448.
21 M. Sun, H. Yu, K. Zhang, S. Wang, T. Hayat, A. Alsaedi and D. Huang, *ACS Sens.*, 2018, **3**, 285–289.
22 L. Yuan, W. Lin, L. Tan, K. Zheng and W. Huang, *Angew. Chem., Int. Ed.*, 2013, **52**, 1628–1630.
23 S. Pal, M. Mukherjee, B. Sen, S. K. Mandal, S. Lohar, P. Chattopadhyay and K. Dhara, *Chem. Commun.*, 2015, **51**, 4410–4413.
24 J. Chan, S. C. Dodani and C. J. Chang, *Nat. Chem.*, 2012, **4**, 973–984.
25 C. Zhang, S. Jin, K. Yang, X. Xue, Z. Li, Y. Jiang, W. Q. Chen, L. Dai, G. Zou and X. J. Liang, *ACS Appl. Mater. Interfaces*, 2014, **6**, 8971–8975.
26 S. Mizukami, *J. Photochem. Photobiol., C*, 2017, **30**, 24–35.
27 X. Zhang, C. Wang, L. Jin, Z. Han and Y. Xiao, *ACS Appl. Mater. Interfaces*, 2014, **6**, 12372–12379.
28 H. W. Yao, X. Y. Zhu, X. F. Guo and H. Wang, *Anal. Chem.*, 2016, **88**, 9014–9021.
29 M. H. Lee, H. M. Jeon, J. H. Han, N. Park, C. Kang, J. L. Sessler and J. S. Kim, *J. Am. Chem. Soc.*, 2014, **136**, 8430–8437.
30 J. R. Lakowicz, D. R. Bevan, B. P. Maliwal, H. Cherek and A. Balter, *Biochemistry*, 1983, **22**, 5714–5722.
31 X. Zhang, C. Wang, L. Jin, Z. Han and Y. Xiao, *ACS Appl. Mater. Interfaces*, 2014, **6**, 12372–12379.
32 P. D. Berk, T. F. Blaschke, B. F. Scharschmidt, J. G. Waggoner and N. I. Berlin, *J. Lab. Clin. Med.*, 1976, **87**, 767–780.
33 L. Y. Chau, *J. Biomed. Sci.*, 2015, **22**, 22.
34 D. Cheng, W. Xu, L. Yuan and X. Zhang, *Anal. Chem.*, 2017, **89**, 7693–7700.
35 L. Yuan and N. Kaplowitz, *Clin. Liver. Dis.*, 2013, **17**, 507–518.
36 J. Zhang, Z. Jin, X. X. Hu, H. M. Meng, J. Li, X. B. Zhang, H. W. Liu, T. Deng, S. Yao and L. Feng, *Anal. Chem.*, 2017, **89**, 8097–8103.
37 J. A. Hinson, D. W. Roberts and L. P. James, Mechanisms of acetaminophen induced liver necrosis, in *Adverse Drug Reactions*, ed. J. Uetrecht, Handbook of Experimental Pharmacology, vol. 196, Springer, Berlin, 2010, pp. 369–405, DOI: 10.1007/978-3-642-00663-0_12.
38 R. R. Nawimanage, B. Prasai, S. U. Hettiarachchi and R. L. McCarley, *Anal. Chem.*, 2017, **89**, 6886–6892.
39 H. W. Liu, X. X. Hu, K. Li, Y. Liu, Q. Rong, L. Zhu, L. Yuan, F. L. Qu, X. B. Zhang and W. Tan, *Chem. Sci.*, 2017, **8**, 7689–7695.
40 Y. Tang, A. Shao, J. Cao, H. Li, Q. Li, M. Zeng, M. Liu, Y. Cheng and W. Zhu, *Sci. China: Chem.*, 2017, **61**, 184–191.
41 P. Li, H. Xiao and B. Tang, *Chin. J. Chem.*, 2012, **30**, 1992–1998.
42 M. C. Yu, Y. Q. Jin, X. Qi, L. J. Bao, Z. S. Qian and C. Q. Zhu, *Chin. J. Chem.*, 2010, **28**, 1165–1170.
43 Z. Guo, S. Park, J. Yoon and I. Shin, *Chem. Soc. Rev.*, 2014, **43**, 16–29.
44 Z. Yang, J. H. Lee, H. M. Jeon, J. H. Han, N. Park, Y. He, H. Lee, K. S. Hong, C. Kang and J. S. Kim, *J. Am. Chem. Soc.*, 2013, **135**, 11657–11662.
45 W. Xu, S. Liu, Q. Zhao, T. Ma, S. Sun, X. Zhao and W. Huang, *Sci. China: Chem.*, 2011, **54**, 1750–1758.
46 K. Gu, Y. Liu, Z. Guo, C. Lian, C. Yan, P. Shi, H. Tian and W. H. Zhu, *ACS Appl. Mater. Interfaces*, 2016, **8**, 26622–26629.
47 Q. Xu, C. H. Heo, G. Kim, H. W. Lee, H. M. Kim and J. Yoon, *Angew. Chem., Int. Ed.*, 2015, **54**, 4890–4894.
48 Y. H. Lee, W. X. Ren, J. Han, K. Sunwoo, J. Y. Lim, J. H. Kim and J. S. Kim, *Chem. Commun.*, 2015, **51**, 14401–14404.
49 S. Xu, H. W. Liu, X. X. Hu, S. Y. Huan, J. Zhang, Y. C. Liu, L. Yuan, F. L. Qu, X. B. Zhang and W. Tan, *Anal. Chem.*, 2017, **89**, 7641–7648.
50 H. M. Kim and B. R. Cho, *Acc. Chem. Res.*, 2009, **42**, 863–872.
51 H. W. Liu, X. B. Zhang, J. Zhang, Q. Q. Wang, X. X. Hu, P. Wang and W. Tan, *Anal. Chem.*, 2015, **87**, 8896–8903.
52 J. Cui, J. Fan, X. Peng, S. Sun, G. Chen and K. Guo, *Sci. China, Ser. B: Chem.*, 2009, **52**, 780–785.
53 T. B. Ren, W. Xu, Q. L. Zhang, X. X. Zhang, S. Y. Wen, H. B. Yi, L. Yuan and X. B. Zhang, *Angew. Chem., Int. Ed.*, 2018, **57**, 7473–7477.
54 H. Li, Q. Yao, F. Xu, N. Xu, X. Ma, J. Fan, S. Long, J. Du, J. Wang and X. Peng, *Anal. Chem.*, 2018, **90**, 4641–4648.
55 Z. Mao, L. Hu, X. Dong, C. Zhong, B.-F. Liu and Z. Liu, *Anal. Chem.*, 2014, **86**, 6548–6554.